Published OnlineFirst September 12, 2014; DOI: 10.1158/0008-5472.CAN-14-0626

Tumor and Stem Cell Biology

Cancer Research

Distinct Subpopulations of Head and Neck Cancer Cells with Different Levels of Intracellular Reactive Oxygen Species Exhibit Diverse Stemness, Proliferation, and Chemosensitivity

Ching-Wen Chang[1], Yu-Syuan Chen[1], Shiu-Huey Chou[2], Chia-Li Han[3], Yu-Ju Chen[3], Cheng-Chieh Yang[4], Chih-Yang Huang[5,6,7], and Jeng-Fan Lo[1,4,5,8,9,10]

Abstract

Head and neck squamous cell carcinoma (HNSCC) is driven by cancer-initiating cells (CIC), but their maintenance mechanisms are obscure. For hematopoietic stem cells, low levels of intracellular reactive oxygen species (ROS^{Low}) is known to help sustain stemness properties. In this report, we evaluated the hypothesis that ROS^{Low} character conferred CIC properties in HNSCC. Sphere cultures define CIC in HNSCC cell populations (HN-CIC). We found that ROS^{Low} cells in HN-CIC defined in this manner were more numerous than in parental HNSCC cells. Further, ROS^{Low} cells frequently coexpressed CIC surface markers such as memGrp78 and Glut3. Exploiting flow cytometry to sort cells on the basis of their ROS level, we found that isolated ROS^{Low} cells displayed relatively more CIC properties, including quiescence, chemoresistance, *in vitro* malignant properties, and tumorigenicity. Pharmacological depletion of ROS modulators in cisplatin-treated HN-CIC reduced CIC properties, enhancing cell differentiation and enhancing cisplatin-induced cell death. Overall, our work defined cell subpopulations in HNSCC on the basis of differential intracellular ROS levels, which associated with stemness and chemoresistance properties. On the basis of our findings, we suggest that strategies to promote intracellular ROS levels may heighten the efficacy of conventional chemotherapy used for HNSCC treatment. *Cancer Res; 74(21); 6291–305. ©2014 AACR.*

Introduction

Emerging evidence supports the hierarchical model of cancer-initiating cells [CIC; also referred to as cancer stem cells (CSC)], in that, each tumor formation is generated from a distinct subset of cells with characteristics of self-renewal and differentiation capacity (1). Clinically, conventional chemotherapeutics generally affect proliferative cells, potentially eliminate proliferating cancer cells but do not target slow dividing cells (2). Like normal tissue stem cells, CICs also exhibit quiescent slow-cycling phenotype (3). In addition, CICs have been shown to be involved in tumor progression, cancer recurrence, and metastasis because of their therapeutic resistance (4, 5). Therefore, to uncover the regulatory physiologic mechanisms that sustain the slow-growing CICs warrants an important study for future therapy development.

Head and neck squamous cell carcinoma (HNSCC) ranks the sixth most common cancer worldwide (6). Previously, we have enriched and identified the existence of a subpopulation of head and neck CICs (HN-CIC) from sphere cells. The enriched HN-CICs from HNSCC cells display both the enhanced properties of stemness and malignancy (7). In addition, the cell surface markers such as CD133 (8) and cell membrane anchoring GRP78 (^{mem}GRP78; ref. 9) for identifying the HN-CICs have also been reported in our previous studies. However, the unique physiology and regulatory mechanisms that mediate the HN-CIC properties of clinical refraction remain elusive. Therefore, the studies on targeting the mechanism(s) in

[1]Institute of Oral Biology, National Yang-Ming University, Taipei, Taiwan. [2]Department of Life Science, Fu-Jen University, New Taipei City, Taiwan. [3]Institute of Chemistry, Academia Sinica, Taipei, Taiwan. [4]Department of Dentistry, School of Dentistry, National Yang-Ming University, Taipei, Taiwan. [5]Graduate Institute of Chinese Medical Science and Institute of Medical Science, China Medical University, Taichung, Taiwan. [6]Institute of Basic Medical Science, China Medical University, Taichung, Taiwan. [7]Department of Health and Nutrition Biotechnology, Asia University, Taichung, Taiwan. [8]Genome Research Center, National Yang-Ming University, Taipei, Taiwan. [9]Department of Dentistry, Taipei Veterans General Hospital, Taipei, Taiwan. [10]National Yang-Ming University VGH Genome Research Center, Taipei, Taiwan.

Note: Supplementary data for this article are available at Cancer Research Online (http://cancerres.aacrjournals.org/).

C.-W. Chang and Y.-S. Chen share first authorship.

Corresponding Authors: Jeng-Fan Lo, Institute of Oral Biology, National Yang-Ming University, No. 155, Section 2, Li-Nong Street, Taipei, 11221, Taiwan. Phone: 886-2-2826-7222; Fax: 886-2-2826-4053; E-mail: jflo@ym.edu.tw; and Chih-Yang Huang, Graduate Institute of Chinese Medical Science and Institute of Basic Medical Science, China Medical University, No 91, Hsueh-Shih Road, Taichung 404, Taiwan. Phone: 886-4-22053366, ext. 3313; Fax: 886-4-22333641; E-mail: cyhuang@mail.cmu.edu.tw

doi: 10.1158/0008-5472.CAN-14-0626

Published OnlineFirst September 12, 2014; DOI: 10.1158/0008-5472.CAN-14-0626

HN-CICs to contribute to the therapeutic resistance of HNSCC would benefit future HNSCC therapy.

Reactive oxygen species (ROS), including superoxide ($O_2^{\bullet}$), hydrogen peroxide (H_2O_2), and the hydroxyl radical ($HO^{\bullet}$), play a major role to cellular proliferation, differentiation, and survival (10). It has recently been shown that stem cells have a unique mechanism, which is important to cope with the accumulated ROS, to increase antioxidant defenses and to play a crucial redox regulator on self-renewal and differentiation, (11–13). For instance, hematopoietic stem cells maintain a low intracellular ROS status that in turn facilitates quiescence, whereas a higher ROS state activates cell proliferation and differentiation but exhausts self-renewal in these cells (14). Achuthan and colleagues (15) demonstrate that drug-induced senescence generates chemoresistant stem-like cells with low ROS in breast cancer. In addition, a lower level of intracellular ROS is also present in breast CSCs, which may contribute to radioresistance (16). Overall, these studies have led to the hypothesis that the maintenance of low ROS levels within the CICs is important for regulating chemoresistance and quiescent state.

Cancer cells are capable of maintained at an oxidation-reduction reactions (redox) homeostasis state by upregulating ROS-scavenging enzymes, which can confer drug resistance (17). Superoxide dismutase (SOD), catalase, glutathione peroxidase, and peroxiredoxin are major intracellular ROS-scavenging enzymes (17). Furthermore, accumulating evidence supports that elevated activity of SOD and catalase is associated with promoting cancer cell resistance to anticancer agents (15, 18, 19).

In this study, we determined the tumorigenic potential and stemness properties of subpopulation cells with the differential intracellular level of ROS in HNSCCs and HN-CICs. We showed that the HN-CICs possessed more ROS^{Low} cells than HNSCCs did. Then, we demonstrated the cells of low level of ROS highly coexpressed the stem cell markers (CD133, ^{mem}Grp78, and Glut3) and the subpopulation of ROS^{Low} cells was expanded in $ALDH^{+}$ cells than in $ALDH^{-}$ cells. Furthermore, three types of cells with differential level of ROS: the high, middle, and low level of ROS (termed "ROS^{High}," "ROS^{Medi}," and "ROS^{Low}") were isolated, respectively. The isolated ROS^{Low} cells displayed CIC properties and possessed high tumorigenicity. Lower ROS level in CICs was also associated with chemoresistance, and pharmacologic depletion of ROS scavengers enhanced the chemosensitivity but diminished the clonogenicity of HN-CICs. In summary, our studies suggest that distinct subpopulation of cells with differential ROS level exerted diverse stemness properties, chemoresistance, and tumorigenicity in HNSCC, and eliminating ROS^{Low} cells should be considered for further exploration on therapeutic development for HNSCC.

Together, abrogation of drug-resistant mechanisms by depletion of ROS scavengers in CICs could have significant therapeutic implications in the future.

Materials and Methods

Cell lines

Human HNSCC cell lines, tongue carcinoma cells (SAS), obtained from the Japanese Collection of Research Bioresources (20) were cultured in DMEM medium with 10% FBS. Human gingival squamous carcinoma cells (OECM-1) were provided from Dr. C.L. Meng (National Defense Medical College, Taipei, Taiwan) and grown in RPMI supplemented with 10% FBS. Cells were cultured at 37°C containing 5% CO_2.

Establishment of the primary cells from patients with HNSCC

This research follows the tenets of the Declaration of Helsinki and all samples were obtained after informed consent from the patients. The clinical samples were approved and in accordance with the Institutional Review Board (IRB no., 2012-07-035BCY), Taipei Veterans General Hospital. Primary HN-CICs were established from patients with HNSCC that derived from specimens of oral surgical resection. The primary HN-CICs were cultured in serum-free DMEM/F12 medium (GIBCO), N2 supplement (GIBCO), 10 ng/mL EGF, and 10 ng/mL human recombinant basic fibroblast growth factor-basic (bFGF; R&D Systems). Otherwise, the primary HNSCCs were cultured in RPMI supplemented with 10% FBS.

Cell lines cultivation and enrichment of HN-CICs

The two cell lines SAS and OECM1 were plated at a density of 7.5×10^4 live cells per 10-mm dish, then cultured in tumor sphere medium consisting of serum-free DMEM/F12 medium (GIBCO), N2 supplement (GIBCO), 10 ng/mL human recombinant bFGF-basic, and 10 ng/mL EGF (R&D Systems). The medium was changed every other day until the tumor sphere formation was achieved to enrich the SAS-HN-CICs or OECM1-HN-CICs in about 4 weeks (7).

Establishment of cisplatin-resistant cell line

The cisplatin-resistant (SAS-$cisPt^R$) cells were generated by serially fractionated exposure of the parental SAS cell lines to cisplatin over a time period of 3 months. At 5 μmol/L of cisplatin killed more than 50% of cells for 48 hours, cells were allowed to recover over 20 days with fresh medium and repeated three times. The cisplatin-resistant (SAS-$cisPt^R$) cells were for further experiments (Supplementary Fig. S1).

Cell viability and chemoresistance assay

Cells were seeded onto 24-well culture plates at 1×10^4 cells per well for 24 hours. Then the test drugs were added to the culture medium for 72 hours. Subsequently, 5 μL of MTT solution (4 mg MTT/mL PBS) was added to each well and the cells were further incubated at 37°C for 3 hours until a purple Formazan was visible. The staining solution was removed and 100 μL DMSO was added at room temperature in the dark for 30 minutes. The absorbance of DMSO solution was detected with a microtiter plate reader at 560 nm. The cell viability ratio is calculated as OD560 of experimental groups/OD560 of control groups.

ROS assay and cell sorting

To detect the intracellular ROS levels, single-cell suspension was resuspended in PBS contain 2% FBS at 10^6 cells/mL, and

Published OnlineFirst September 12, 2014; DOI: 10.1158/0008-5472.CAN-14-0626

stained with 10 μmol/L DCF-DA, 5 μmol/L CM-H2DCFDA, 2.5 μmol/L CellROX Deep Red, or 5 μmol/L Carboxy-DCFDA (Invitrogen) at 37°C for 30 minutes, respectively. Cells were washed and resuspended in 10 μmol/L propidium iodide (PI) solution for analysis or sorting by using FACSAria cell sorter (Becton Dickinson). For all FACS experiments, the dead cells were excluded by PI staining.

Anchorage-independent growth assay

Each well (35 mm) of a 6-well culture dish was coated with 2 mL bottom agar (Sigma-Aldrich) mixture [DMEM, 10% (v/v) FBS, 0.6% (w/v) agar]. After the bottom layer was solidified, sorted cells were cultured in 2 mL top agar medium mixture [DMEM, 10% (v/v) FBS, 0.3% (w/v) agar], and the dishes were incubated for 2 weeks at 37°C. Subsequently, plates were stained with 0.005% Crystal Violet then the colonies were counted. The number of total colonies was counted over five fields per well for a total of 15 fields in triplicate experiments.

In vivo tumorigenic assay

All animal studies were approved and in accordance with the Institutional Animal Care and Use Committee (IACUC) of National Yang-Ming University (Taipei, Taiwan; IACUC approval no., 1001223). Equal volume of cells and Matrigel (BD Biosciences) were mixed and s.c. injected into the back of nude mice (6–8 weeks). Tumor volume was calculated using the following formula: (Length × Width^2)/2.

Results

Quantification of intracellular ROS level and coexpression of CIC surface markers in parental HNSCCs cells, sphere cells, and primary cells established from HNSCC tumor tissue

It has been demonstrated that cells with low intracellular ROS concentration are more likely to maintain their stem properties in hematopoietic stem cells (14). In addition, the association of low ROS level and radioresistance in breast CSCs has been reported (16). Previously, we have successfully enriched a subpopulation of HN-CICs derived from both SAS and OECM1 HNSCCs (7, 9). Herein, we first aim to understand whether the intracellular level of ROS is relatively lower in HN-CICs. To measure the intracellular ROS level of HN-CICs, the cells were stained with oxidation sensitive fluorescent probe (DCFDA, CM-DCFDA, or CellROX Deep Red, respectively) followed by flow-cytometry analysis (14, 16). Compared with parental HNSCCs, we observed that a subpopulation of cells with low intracellular level of ROS was significantly increased in HN-CICs (for both SAS-S and OECM1-S; Fig. 1A and B and Supplementary Fig. S2A). In addition, primary cells (primary-S) freshly established from HNSCC patient tumor tissue grown in defined serum-free medium with bFGF and EGF growth factors (the medium to grow the SAS-S and OECM1-S cells) also displayed more cells with low ROS content in comparison with the same cells cultivated in medium supplied with 10% FBS (primary-P; the medium to grow the SAS-P and OECM1-P cells; primary-S, 12.2% vs. primary-P, 4.3%; Fig. 1A). We next sought to determine whether the fluorescence change were attributable to be altered by the dye oxidation and not altered by uptake, ester cleavage, or efflux of the probe. As shown in Supplementary Fig. S2B, these results demonstrated that no significant difference of SAS-P and SAS-S cells on staining of the oxidation-insensitive analog of Carboxy-DCFDA as the negative control (Supplementary Fig. S2B; ref. 21).

Our previous data demonstrate that both ^{mem}GRP78 and CD133 could be used as a surface marker for enrichment of HN-CICs (8, 9). Next, we wanted to determine whether there was a positive correlation between the lower level of ROS and the abovementioned CIC surface markers of HN-CICs. Examined by FACS analyses, the HN-CICs showed elevated coexpression of either ^{mem}GRP78 or CD133 with lower level of ROS in comparison with the parental HNSCCs (Fig. 1C and D). Furthermore, the expression of Glut3, a recently identified cell surface marker of brain tumor stem cells (22), was also highly correlated with the cells containing low intracellular ROS amount (Fig. 1E). Finally, it has been shown that cells harboring higher aldehyde dehydrogenase (ALDH) activity display the characteristics of CSCs (23). As expected, the sorted ALDH$^+$ cells also displayed more low ROS cells than the sorted ALDH$^-$ cells in HNSCCs (Fig. 1F). To further clarify the correlation between ALDH activity and representative CIC markers of cells, SAS sphere cells or cisplatin-resistant SAS cells (SAS-cisPt^R) were selectively double stained with CD133/Glut3 or Grp78/Glut3. The ALDH activity of the double-stained cells was also examined by ALDEFLUOR assay. Interestingly, we found that cell subpopulation positively double stained with the selected CIC markers (such as the CD133$^+$Glut3$^+$ or ^{mem}Grp78$^+$Glut3$^+$ subpopulation) also contained the highest level of ALDH activity in comparison with the rest individual subpopulations (Supplementary Fig. S1). The abovementioned observation suggests that the ALDH$^+$ subpopulation cells mainly overlap with the same subpopulation of cells that are Grp78$^+$CD133$^+$Glut3$^+$ in HNSCC cells. Collectively, these results suggest that lower level of ROS is closely related to cancer stemness properties in HN-CICs.

Interestingly, we also observed a subpopulation of cells containing higher level of endogenous ROS in HN-CICs (Fig. 1G). The high ROS level may be reflective of an "activated" state to mimic the proliferative activity of progenitor cells in neural stem cells (24). Characterization of the ROS^{High} cells was further examined (see text later).

ROS^{Low} cells display CIC properties

To characterize the CIC properties of cells with differential level of intracellular ROS amount, we stained the HN-CICs with ROS-indicator dye DCFDA to separate cells into ROS^{Low}, ROS^{Medi}, and ROS^{High} subpopulations followed by flow cytometry (Fig. 2A), and the stemness properties of the three isolated cell subpopulations were further assessed. Initially, we observed that the ROS^{Low} cells maintained a spheroid-growing phenotype; however, both the ROS^{Medi} and ROS^{High}

Published OnlineFirst September 12, 2014; DOI: 10.1158/0008-5472.CAN-14-0626

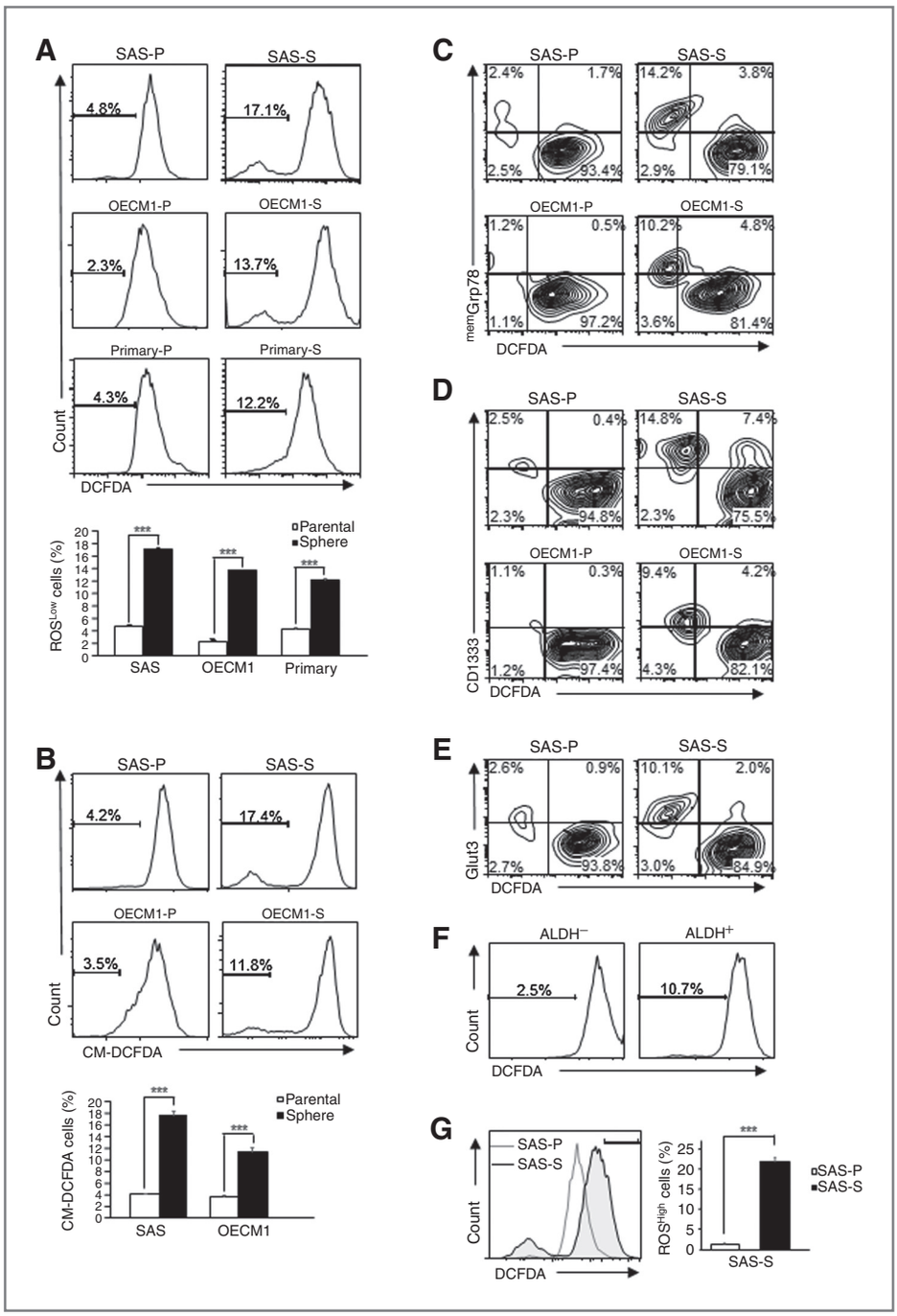

Figure 1. Quantification of intracellular ROS level and coexpression of CSC surface markers in parental HNSCCs cells (SAS-P and OECM1-P), sphere cells (SAS-S and OECM1-S, derived from parental HNSCCs), and primary cell lines established from HNSCC patient tumor tissue. A, single-cell suspension from parental HNSCCs, sphere cells, or primary HNSCC cells was stained with DCFDA. Then, the intracellular level of ROS in parental HNSCCs, sphere cells, and primary cells was determined by FACS analyses. B, the percentage of CM-DCFDA^{+} cells in parental HNSCCs and sphere cells was analyzed by flow cytometry. The coexpression profile between low ROS level and ^{mem}Grp78 (C), CD133 (D), and Glut3 (E) in HNSCCs and sphere cells was examined by FACS. [P, parental HNSCCs; S, HNSCC-derived sphere cells; primary-P, primary HNSCC cultivated in serum containing medium; primary-S, primary HNSCC cells cultivated in defined medium without FBS (details seen in Materials and Methods)]. F, the percentage of low ROS level cells in isolated ALDH1^{+} and ALDH1^{-} HNSCCs, respectively. G, quantification of ROS^{High} cells was determined by coplotting the expression profile of ROS content of SAS-P and SAS-S cells stained by DCFDA and analyzed by flow cytometry. Results, means ± SD of triplicate samples from three experiments (***, $P < 0.001$).

cells grew as an adherent phenotype under the cell culture condition containing 10% FBS (Fig. 2B). Furthermore, the freshly isolated ROS^{Low}, ROS^{Medi}, and ROS^{High} cells were cultivated within the medium containing 10% FBS for 5 days; afterward, the intracellular ROS level of the cultivated cells was analyzed, respectively. We observed that the ROS^{Low} cells remained as ROS^{Low} cells, whereas cells with a low level of ROS were not detectable from the further cultivated ROS^{Medi} and ROS^{High} subpopulation cells by FACS analyses (Fig. 2C).

In addition, the expression level of stemness genes (Oct4 and Nanog) within the ROS^{Low}, ROS^{Medi}, and ROS^{High} cells was examined transcriptionally and translationally. As shown in Fig. 3A and B, we observed enhanced expression of mRNA transcript and protein level of stemness genes (Oct4 and Nanog) in ROS^{Low} cells in comparison with those of ROS^{Medi} and ROS^{High} cells, respectively. Next, we performed tumor spheres formation assay for evaluating the self-renewal ability of ROS^{Low}, ROS^{Medi}, and ROS^{High} cells. Again, the ROS^{Low} cells

Published OnlineFirst September 12, 2014; DOI: 10.1158/0008-5472.CAN-14-0626

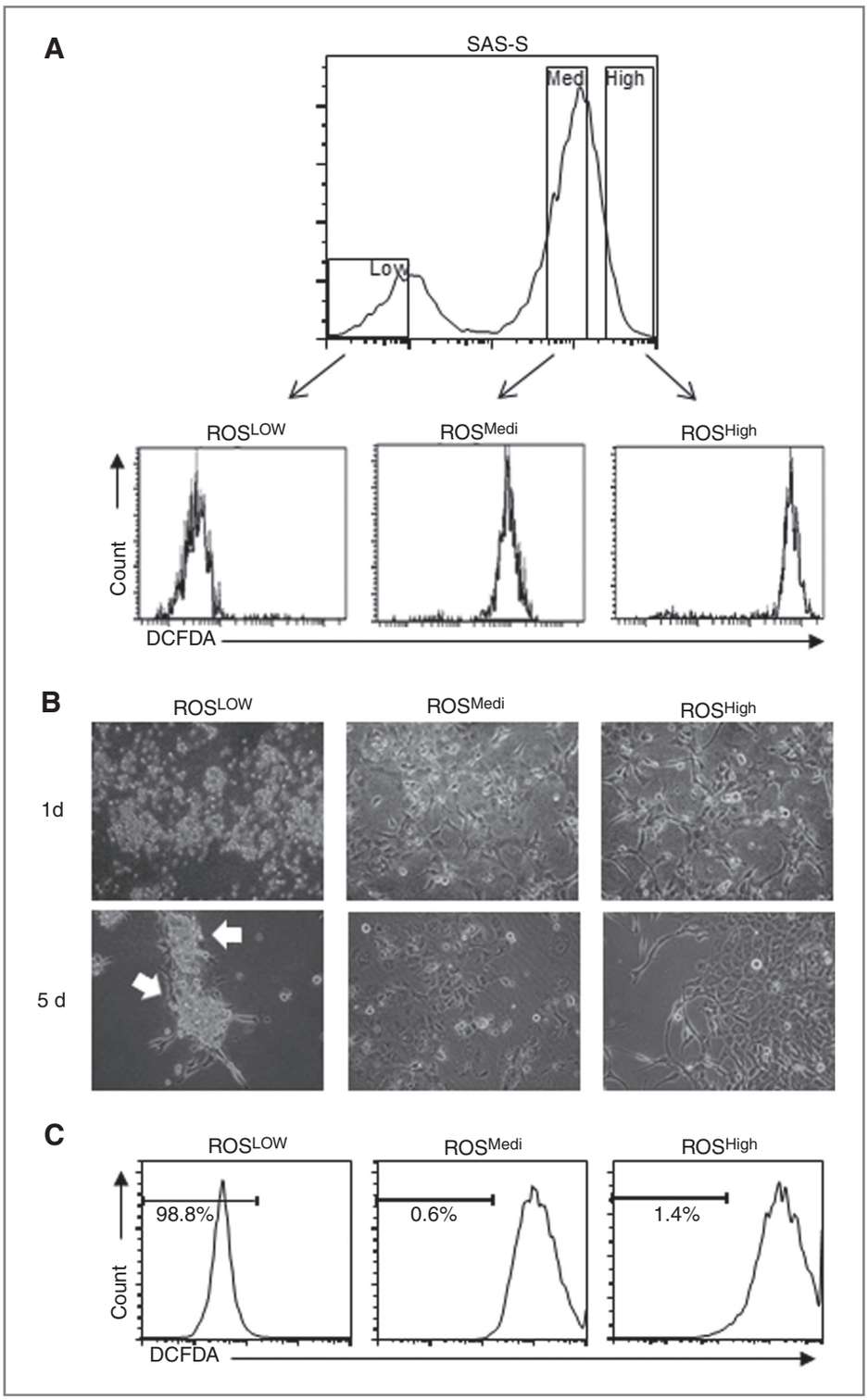

Figure 2. Isolation of ROS^{Low}, ROS^{Medi}, and ROS^{High} cells. A, ROS^{Low}, ROS^{Medi}, and ROS^{High} cells were sorted using DCFDA staining as the intracellular ROS indicator from SAS sphere cells. B, representative images of freshly sorted ROS^{Low}, ROS^{Medi}, and ROS^{High} cells, grown under standard medium containing 10% FBS for 1 and 5 days, were shown by phase contrast microscopy (arrow, spheroids). C, at day 5, the intracellular ROS content of further cultivated ROS^{Low}, ROS^{Medi}, and ROS^{High} cells was reanalyzed by flow cytometry.

displayed better sphere-forming capability than ROS^{Medi} and ROS^{High} cells did (Fig. 3C). Of note, the ROS^{High} cells displayed an intermediate sphere-forming ability (Fig. 3C and Supplementary Fig. S3A).

In reference to stem cell phenotype, stem cell can be further identified by property of smaller cell size (25–27). Additional evidence also suggests that terminally differentiated keratinocytes progressively increase their cell size during human

Published OnlineFirst September 12, 2014; DOI: 10.1158/0008-5472.CAN-14-0626

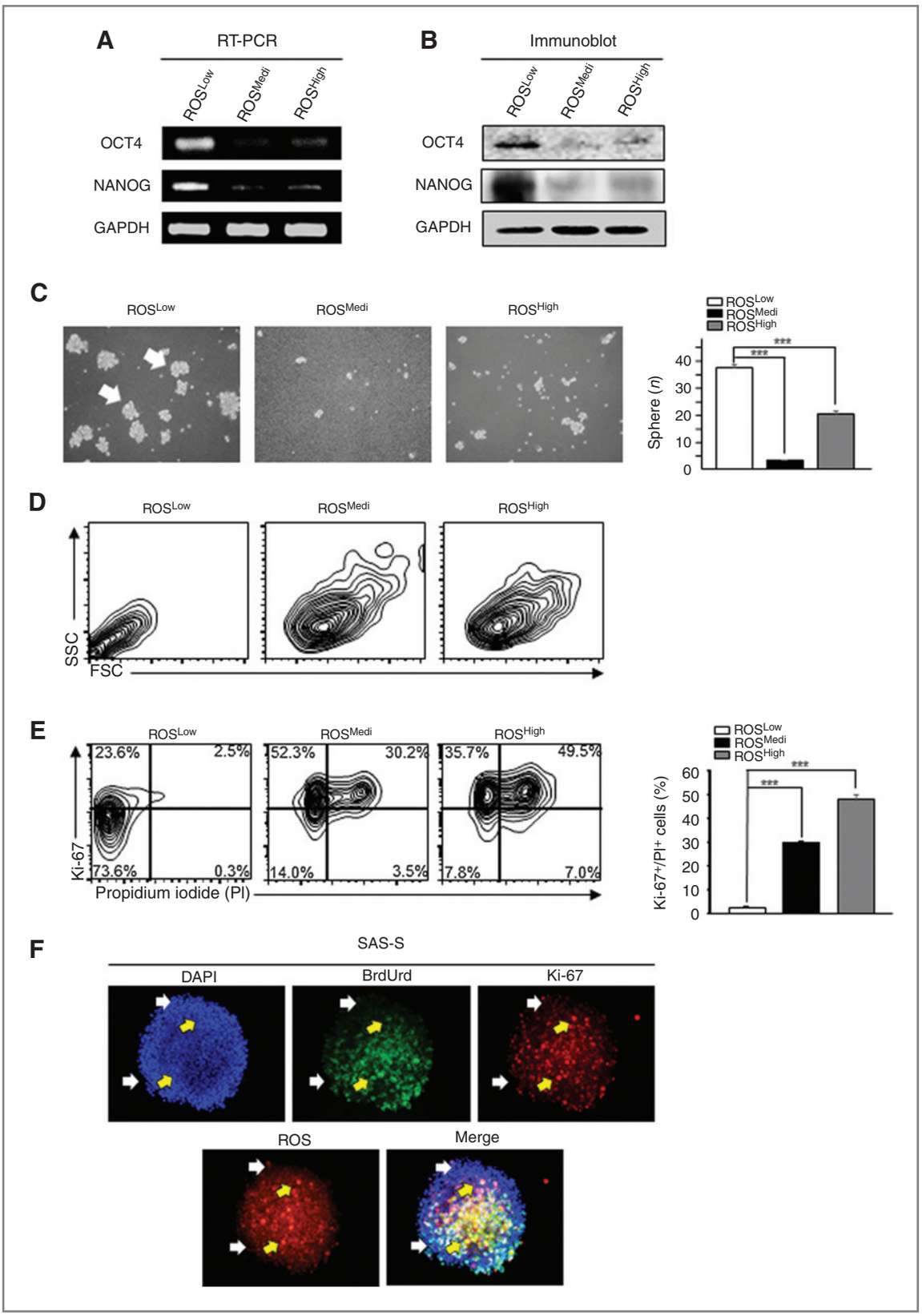

Published OnlineFirst September 12, 2014; DOI: 10.1158/0008-5472.CAN-14-0626

keratinocyte maturation (28). We therefore analyzed cell size of ROS^{Low}, ROS^{Medi}, and ROS^{High} cells by physical parameters forward and side scatter (FSC, cell size and SSC, cell granularity). As shown in Fig. 3D, the size of ROS^{Low} cells was smaller than that of ROS^{Medi} and ROS^{High} cells.

A low endogenous ROS status of HNSCCs maintains the quiescent state of CICs

Stem cells are present in a quiescent state but are able to exit quiescence by ROS activation; in addition, the quiescent state appears to be necessary for retaining the self-renewal of stem cells, and is a critical factor in the resistance of CICs to chemotherapy and targeted therapies (29). Next, we sought to determine whether the sorted ROS^{Low} cells possess the abovementioned stem cell perspectives. To assess the quiescent state of cells, we performed cell-cycle analysis by double staining the cells with proliferative marker Ki-67 and PI for DNA content. As expected, we found that the sorted ROS^{Low} cells were present in a relatively quiescent state (Ki-67^{+}/PI^{+}, 2.5%), whereas the sorted ROS^{High} cells displayed the highest percentage of proliferative activity (Ki-67^{+}/PI^{+}, 49.5%; Fig. 3E). The above observation was further confirmed by immunoblotting with the cell-cycle exit index [BrdUrd (bromodeoxyuridine) and Ki67]. As shown in Fig. 3F, we discovered that the sphere cells expressing high oxidative state (yellow arrows) exhibited a significantly higher proliferative activity in comparison with the cells expressing lower oxidative state (white arrows). We next sought to determine whether increasing of intracellular superoxide level by NADPH oxidase activation could trigger cell-cycle entry of the quiescent ROS^{Low} cells, which were largely resided in sphere cells? Strikingly, the sphere cells treated with NADPH oxidase activator H_2O_2 (30) or arsenic (31) displayed more adhesive cells but less sphere cells under microscopic observation (Supplementary Fig. S3B). These data indicate that the low ROS state is associated with the quiescent state of stem cells; on the contrary, the high ROS state is correlated with proliferative activity in HNSCCs.

ROS^{Low} cells show enhanced malignant potentials *in vitro* and *in vivo*

To evaluate the differential malignancy among ROS^{Low}, ROS^{Medi}, and ROS^{High} cells, the *in vitro* anchorage-independent growth ability and the *in vivo* xenografts assay were performed. The sorted ROS^{Low} cells significantly grew larger and more colonies than the ROS^{Medi} cells and ROS^{High} cells did in soft agar (Fig. 4A). *In vivo*, the ROS^{Low} cells also showed the best tumor-initiating ability, being able to form tumor with only 500 inoculated cells, whereas the ROS^{High} cells needed at least 1×10^4 cells to grow the tumors, which concludes that the ROS^{Low} cell is 20-fold more tumorigenic than the ROS^{High} cells. Nevertheless, the ROS^{Medi} cells did not generate any tumors under the examined conditions (from 5×10^2 to 1×10^4 cells; Fig. 4B and C).

To further verify the hypothesis that low level of ROS is pivotal for maintenance of cancer stemness properties and responsible for tumor growth in nude mice, the stemness properties within the newly established primary cells derived from ROS^{Low}- and ROS^{High}-generated tumors were further analyzed, respectively (see Materials and Methods for establishment of primary cells from xenografted tumors). In the beginning, the newly established primary culture cells derived from ROS^{Low}-generated tumor formed spheroids promptly. Empirically, after 3 days of cultivation, the sphere cells became adherent when the nonserum culture condition was switched to DMEM medium containing 10% serum (Fig. 4D). However, we did not observe any spheroid formation from the primary culture cells, which were derived from tumors generated by ROS^{High} cells. Interestingly, the primary culture cells established from ROS^{Low}-derived tumors kept more ROS^{Low} cells (11.5%) than the cells established from ROS^{High}-derived tumors did (7.3%; Fig. 4E). In addition, we observed more ^{mem}GRP78-positive cells in primary culture cells established from ROS^{Low}-derived tumors (10.0%) than the cells established from ROS^{High}-derived tumors (5.5%; Fig. 4F).

Collectively, these results suggest that the sorted ROS^{Low} cells are more tumorigenic and possess CIC properties in comparison with the ROS^{High} and ROS^{Medi} cells.

HN-CICs are more chemoresistant and cisplatin treatment enriches the ROS^{Low} cells

To further understand whether HN-CICs are more chemoresistant than the HNSCC cells, we examined the cytotoxic effect of cisplatin treatment on both HNSCC and sphere cells with enriched HN-CICs. Being treated with cisplatin for 72 hours, both the parental SAS and OECM1 cells gave an IC_{50} value of around 7.5 μmol/L; however, the SAS sphere cells or OECM1 sphere cells showed a similar IC_{50} value of more than 20 μmol/L to the cisplatin treatment (Fig. 5A). Furthermore, the SAS sphere cells displayed an enhancement of ROS^{Low} cells in a dose-dependent manner under cisplatin treatment (Fig. 5B). In addition, we found an approximately 4-fold reduction in the percentage of ROS^{High} cells in the cisplatin treatment group versus the untreated group (Fig. 5C; untreated: 20% vs. cisplatin treated: 5%), suggesting that ROS^{High} cells are relatively chemosensitive in comparison with ROS^{Low} cells, in SAS sphere cells.

Cancer stem properties are enhanced during the selection of cisplatin resistance in HNSCC (32). To further evaluate the

Figure 3. Stem cell properties and physiologic characteristics of ROS^{Low}, ROS^{Medi}, and ROS^{High} cells. Expression of pluripotent stemness genes (Oct4 and Nanog) in ROS^{Low}, ROS^{Medi}, and ROS^{High} cells was determined by qRT-PCR (A) and immunoblot analyses (B). The amount of GAPDH was referred as loading control. C, representative images of tumor sphere–forming ability of ROS^{Low}, ROS^{Medi}, and ROS^{High} cells grown under defined serum-free selection medium are shown. The numbers of tumor spheres were further calculated using microscope. D, representative plots according to the size (FSC) and structure (SSC) of the sorted ROS^{Low}, ROS^{Medi}, and ROS^{High} cells were shown by FACS analyses. E, the proliferative activity of sorted ROS^{Low}, ROS^{Medi}, and ROS^{High} cells was stained with Ki-67/PI and further analyzed by flow cytometry. Results, means ± SD from three experiments (***, $P < 0.001$). F, intracellular localization of BrdUrd labeling (green) and Ki-67 (red); and content of ROS (orange) was determined by immunofluorescence staining. Nuclei were stained with DAPI (blue; yellow arrows, ROS^{High} cells; white arrows, ROS^{Low} cells).

Published OnlineFirst September 12, 2014; DOI: 10.1158/0008-5472.CAN-14-0626

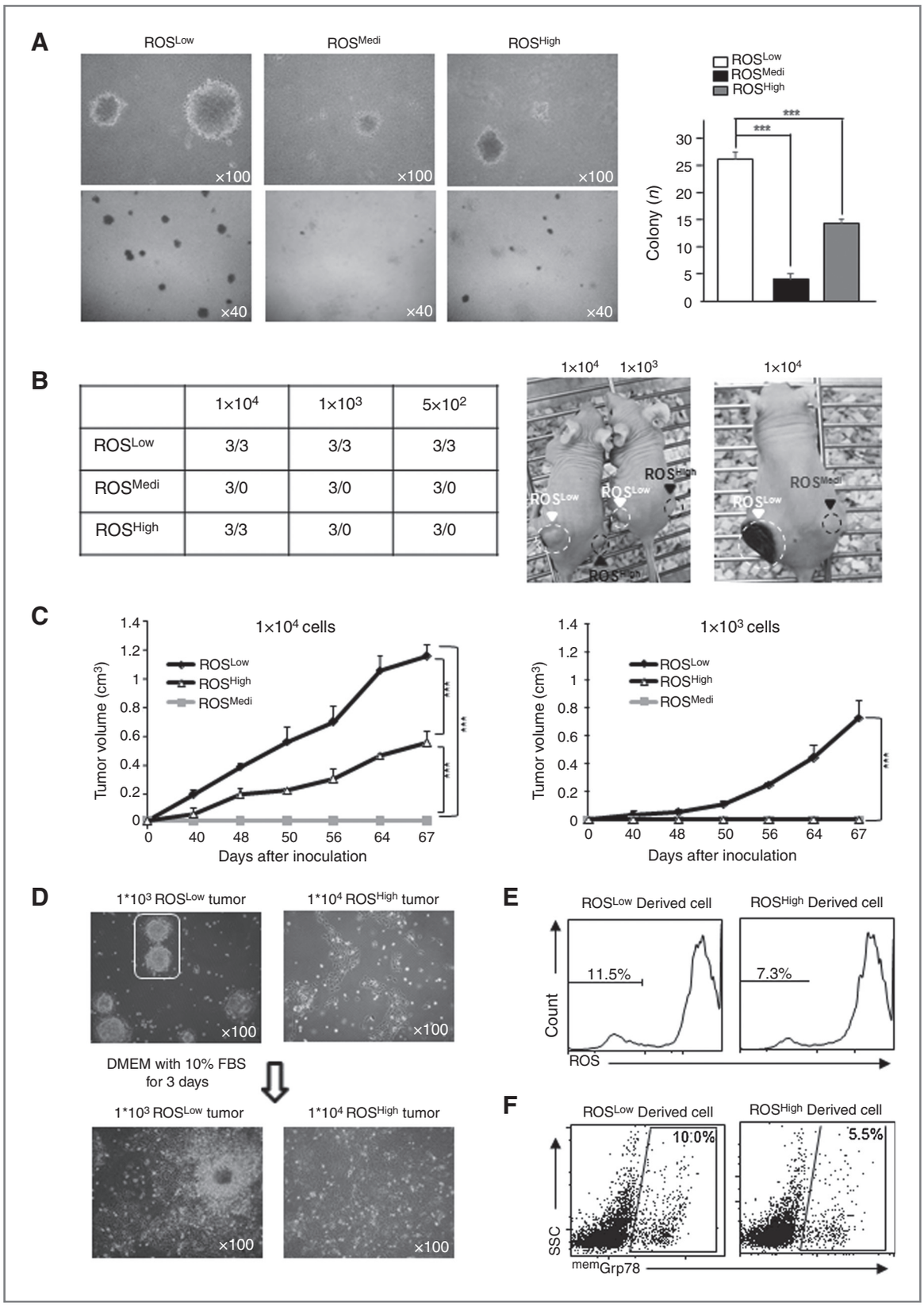

Published OnlineFirst September 12, 2014; DOI: 10.1158/0008-5472.CAN-14-0626

correlation between low ROS level and cancer stemness properties, we established a cisplatin-resistant HNSCC cell line (SAS-cisPt^{R}) from SAS cells by progressive cisplatin treatment (Supplementary Fig. S4; and see details from Materials and Methods). Obviously, the cell subpopulation with low level of ROS was significantly enhanced in cisplatin-resistant HNSCCs (SAS-cisPt^{R}; Fig. 5D). It has also been shown that cells harboring higher ALDH activity display the characteristics of CSCs (23). Therefore, we wanted to understand the relationship between ALDH activity and cisplatin resistance in HNSCCs. Empirically, we found that SAS-cisPt^{R} cells increased the percentage of ALDH-positive (ALDH^{+}) cells (Fig. 5E).

ROS scavenging and pharmacologic modulation of ROS level affect the chemosensitivity of HN-CICs

In light of recent findings that conventional chemotherapy may not be in sufficient effect, in which the increased expression of ROS defense genes is accompanied within CICs (16, 33, 34). Given our observations of HN-CICs containing more ROS^{Low} cells, we proposed that these cells may possess elevated level of ROS-scavenging enzymes compared with HNSCCs. Therefore, we compared the expression profile of ROS scavenger genes of the enriched HN-CICs (from SAS to OECM1) with that of parental cells (SAS and OECM1) by Affymetrix microarray analyses. As noticed, the transcripts of some ROS scavenger genes were upregulated in enriched HN-CICs (Fig. 5F and Supplementary Fig. S5). Furthermore, this Affymetrix microarray analysis showed significant increasing trend of superoxide dismutase 2 (SOD2), catalase (CAT), and peroxiredoxin 3 (PRDX3) in the enriched HN-CICs (Fig. 5F). Both SOD2 and CAT are antioxidant enzymes, and are associated with regulation of cellular ROS and the acquired drug resistance in cancer (15, 17, 35). Consistent with microarray results, RT-PCR analyses showed that the expression of SOD2 and CAT transcript was increased in enriched HN-CICs than that in parental HNSCCs (Fig. 5G). Furthermore, the catalase enzymatic activity of HNSCC and HN-CICs was measured by catalase activity assay. As shown in Supplementary Fig. S6, HN-CICs exhibited a higher catalase activity as compared with HNSCC. However, we did not see significant difference of the PRDX3 transcript among the HN-CICs and HNSCCs (Fig. 5G). We observed that low ROS level was in association with upregulation of antioxidant enzymes such as SOD2 and CAT in HN-CICs (Fig. 5G). Next, we aimed to pharmacologically inhibit or genetically diminish the activity of ROS scavenger enzymes, then to abrogate the chemoresistance and stemness properties of CICs. Pharmacologic and genetic inhibition of SOD2 or catalase, respectively, both reduced the ROS^{Low} subpopulation cells in SAS sphere cells (Fig. 5H; around 8%; Supplementary Fig. S7A and S8A). In opposite, single cisplatin treatment enhanced the ROS^{Low} cell subpopulation in HN-CICs (Fig. 5H; 22% and Supplementary Fig. S7A). However, combined treatment with cisplatin plus 2-methoxyestradiol (2-ME) or 3-amino-1,2,4-triazole (3AT) significantly lowered the ROS^{Low} cell subpopulation compared with single treatment with cisplatin in HN-CICs (Fig. 5H; and Supplementary Fig. S7A). Furthermore, triple treatment with 2-ME, 3-AT plus cisplatin showed the most significant effect on reducing the ROS^{Low} cell subpopulation in HN-CICs (Fig. 5H; around 2% and Supplementary Fig. S7A). Next, we wanted to address whether SOD2 and/or CAT inhibition in combination with/without cisplatin treatment would reduce the cell viability in HN-CICs. As shown in Fig. 6A, the cell viability of CICs singly or combinatorially treated with 2-ME, 3-AT, and/or cisplatin was analyzed by MTT assay. Along with the reduction of ROS^{Low} cell subpopulation in HN-CICs under triple treatment of 2-ME, 3-AT plus cisplatin (Fig. 5H), we also observed that the cell viability of the triple-treated HN-CICs was the most significantly diminished (left with around 35%) by MTT assay (Fig. 6A).

Finally, to further examine whether pharmacologic modulation of ROS levels contributed to cell death in HN-CICs, SAS sphere cells were singly or combinatorially treated with 2-ME, 3-AT, or cisplatin. The treated cells undergoing cell death was determined by costained with Annexin V and PI and examined by flow cytometry. Single treatment of 2-ME or 3-AT caused a slight increase in cell death of HN-CICs. In addition, combined treatment with 2-ME or 3-AT sensitized the cytotoxicity of cisplatin treatment in HN-CICs. Moreover, triple treatment with 2-ME and 3-AT plus cisplatin was the most effective and induced around 45% of the cell population undergoing cell death (Fig. 6B and Supplementary Fig. S7B). Together, these data demonstrate the importance of antioxidant defense to maintain the low ROS level, cell viability, and chemosensitivity of HN-CICs

Antioxidant ability is required to maintain the stemness properties and malignancy of HN-CICs

To further evaluate whether the antioxidant ability is important to sustain the stemness properties of HN-CICs, the SAS sphere cells were treated with 2-ME, 3-AT, or cisplatin alone or in combination. As shown in Fig. 6C, the sphere cell singly treated with 2-ME or 3-AT displayed decreased expression of "cancer stemness" proteins (Oct-4 and Nanog). In opposite, we observed that sphere cell singly treated with cisplatin showed

Figure 4. Distinct *in vitro* malignancy and *in vivo* tumorigenic properties of ROS^{Low}, ROS^{Medi}, and ROS^{High} cells. A, to elucidate the anchorage-independent growth ability, single cells suspension of ROS^{Low}, ROS^{Medi}, and ROS^{High} cells was plated onto soft agar and further analyzed. B, summary of the *in vivo* tumor growth ability of sorted ROS^{Low}, ROS^{Medi}, and ROS^{High} cells examined by xenotransplantation analyses (left). Representative tumors, which were generated by inoculating the ROS^{Low}, ROS^{Medi}, and ROS^{High} cells into the subcutaneous space of recipient nude mice, were recorded on day 56, respectively (right). C, tumor growth curves were measured after inoculation of ROS^{Low}, ROS^{Medi}, and ROS^{High} HNSCCs subcutaneously into nude mice (left, 1×10^4 cells; right, 1×10^3 cells). D, growth pattern of primary culture cells, which were derived from ROS^{Low} or ROS^{High} cell generated tumors, respectively, cultured under standard medium containing 10% serum. In the beginning, primary cells derived from ROS^{Low} tumor formed spherical clusters of cells. In opposite, ROS^{High} tumor–derived cells immediately attached to the culture dish (top). After incubation for 3 days, the ROS^{Low} tumor–derived cells were proliferative from spherically aggregated cell clusters (bottom). The expression profile of the intracellular ROS content (E) and ^{mem}Grp78 (F) of newly established cell lines, which were derived from ROS^{Low}- and ROS^{High}-xenografted tumors, was examined by FACS analyses, respectively. Error bars correspond to SD. Results, means ± SD of triplicate samples from three experiments ($n = 3$; ***, $P < 0.001$).

Published OnlineFirst September 12, 2014; DOI: 10.1158/0008-5472.CAN-14-0626

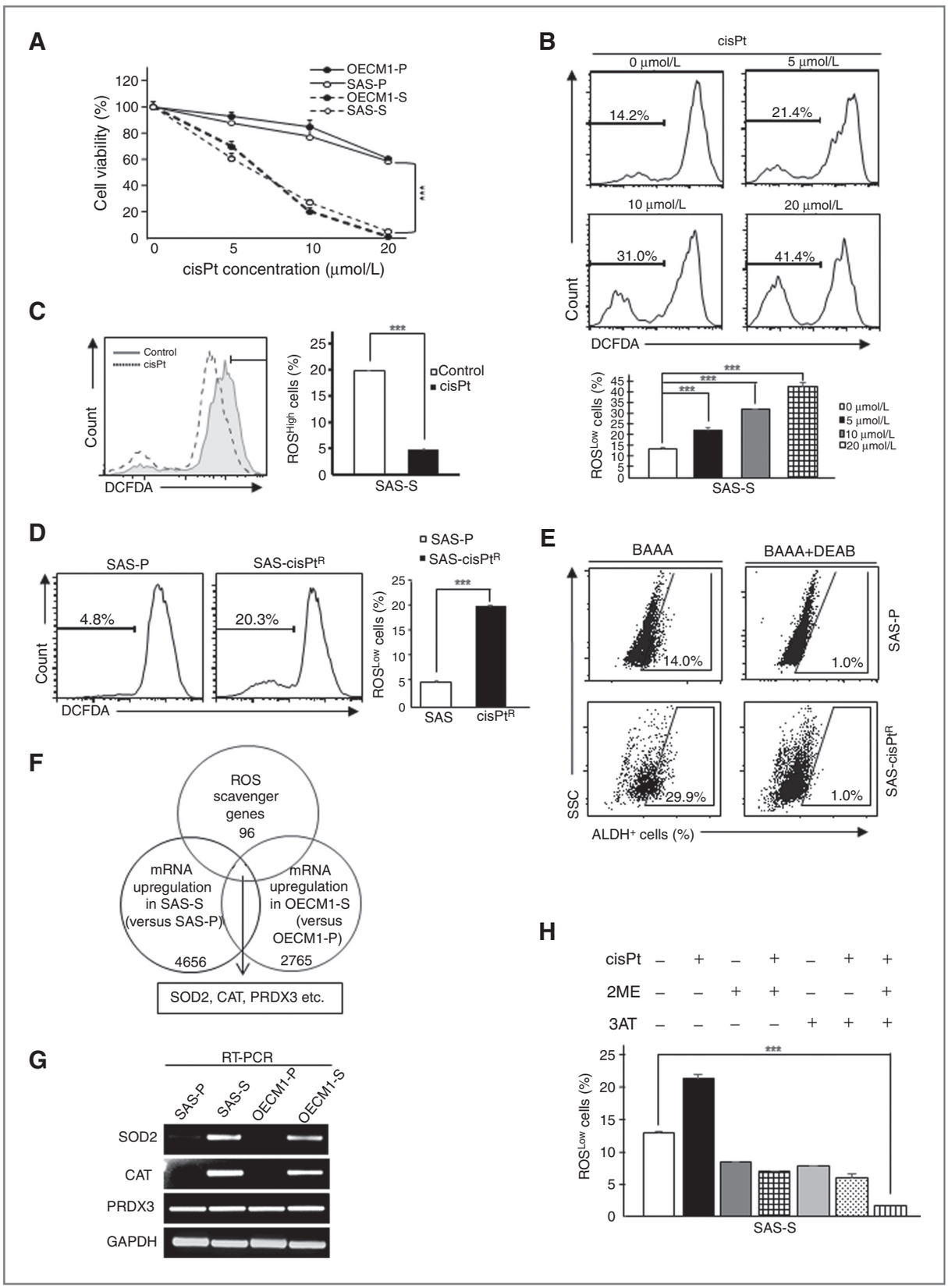

Published OnlineFirst September 12, 2014; DOI: 10.1158/0008-5472.CAN-14-0626

higher protein levels of Oct-4 and Nanog but did not affect the expression of epithelial differentiation marker, cytokeratin 18 (CK-18) and Involucrin (Fig. 6C–E and Supplementary Fig. S7C). However, pharmacologic and genetic inhibition of SOD2 or catalase caused the increase of CK18$^+$ subpopulation cells but the decreased expression of CIC marker CD44 in HN-CICs (Fig. 6D, Supplementary Fig. S8B and S8C). In addition, the sphere/anchorage-independent colony formation abilities of HN-CICs under genetic inhibition of SOD2 or catalase were also significantly abolished (Supplementary Fig. S8D and S8E). Interestingly, HN-CICs undergoing pharmacologic or genetic inhibition of catalase rather than inhibition of SOD2 displayed a more potent efficiency to cause the cell differentiation (Fig. 6D; 3-AT, 40%; 2-ME, 20%; Fig. 6E and Supplementary Fig. S8B). Nevertheless, the triple treatment of 3-AT, 2-ME plus cisplatin showed the most potential to enhance the CK18-positive cells (Fig. 6D; around 56% and Fig. 6E). In the mean times, triple treatment of 3-AT, 2-ME plus cisplatin significantly inhibited the sphere formation ability of HN-CICs, whereas relatively larger size spheres were observed from single cisplatin-treated HN-CICs (Fig. 6F).

We next sought to determine whether inhibition of the activity of ROS scavenger enzymes could attenuate the malignancy of HN-CICs both *in vitro* and *in vivo*. As shown in Fig. 6G, the anchorage-independent growth abilities of SAS sphere cells under triple treatment were significantly abolished. In addition, triple treatment of 3-AT, 2-ME plus cisplatin to SAS sphere cells or SAS-cisPt^R cells significantly reduced the tumor volumes by xenograft transplantation assay (Fig. 6H and I). Overall, combined treatment with 2-ME and 3-AT reduced the self-renewal ability of HN-CICs, and sensitized the *in vitro* cytotoxicity mediated by cisplatin treatment on HN-CICs.

Catalase has been reported to be highly correlated with tumor malignant grade (36). We therefore proceeded to evaluate whether overexpression of catalase could enhance stemness properties. Treatment of SAS sphere cells with PEG-CAT displayed not only elevated expression of catalase activity but also the increased percentage of ROS^{Low} cells (Supplementary Fig. S9A and S9B). Furthermore, we demonstrated that catalase overexpression also resulted in increased expression of CIC markers (^{mem}Grp78, CD44, and ALDH activity). (Supplementary Figs. S9C, S9D, and S10A). To further understand whether treatment of cisplatin, 3-AT or 2-ME can cause significant cytotoxicity to normal stem cells, the hematopoietic stem cells (HSC) were first treated with the above drugs and subjected to MTT assay, respectively. We observed that single treatment of cisplatin or 2-ME decreased the cell viability of HSC cells. However, there was no significant inhibition of cell viability on 3-AT–treated HSC cells (Supplementary Fig. S11).

Discussion

Patients with HNSCC are still very likely to relapse within months after therapy (37) that may be because conventional treatments cannot efficiently eliminate CICs, which are involved in the tumor progression, metastasis, and chemo/radio resistance (2). Most of the anticancer drugs kill cancer cells by induced ROS generation, but prolonged treatment with the drugs results in reduced ROS level as a result of therapy resistance (38, 39). Caraglia and colleagues (40) provide evidence that the determination of oxidative stress status could be a marker of drug efficacy in patients with cancer. Thus, we hypothesized CICs are resistant to therapies due to their lower intracellular ROS content compared with the differentiated cancer cells. Moreover, understanding the relationships between ROS and drug resistance of CICs is important to improving the efficacy for future chemotherapies.

In the present study, we show that HN-CICs contain lower concentrations of ROS than parental cancer cells. Consequently, cell subpopulations, including ROS^{Low}, ROS^{Medi}, and ROS^{High} with differential ROS level, were isolated. Notably, ROS^{Low} cancer cells are closely associated with CD133, ^{mem}Grp78, Glut3, and ALDH$^+$ cells (Fig. 1). We observed that the ROS^{Low} cells displayed a sphere-growing phenotype; in contrast, both the ROS^{Medi} and ROS^{High} cells grew as an adherent phenotype under the same culture condition (Fig. 2). Furthermore, ROS^{Low} HN-CIC cells displayed CIC properties in comparison with ROS^{Medi} and ROS^{High} subpopulation cells. Furthermore, cell-cycle studies indicated that ROS^{Low} cells existed in lower Ki-67 activity (Fig. 3). Importantly, an *in vivo* nude mice model demonstrates that ROS^{Low} population possessed high tumorigenic potential (Fig. 4). In addition, HN-CICs seem able to regulate ROS to exhibit chemoresistance by increasing production of antioxidant genes (Fig. 5). Pharmacologic depletion of ROS scavengers in CICs reduced their clonogenicity and resulted in chemosensitization to cisplatin both *in vitro* and *in vivo* (Fig. 6). Collectively, our data first demonstrated the crucial role of low ROS level for the tumorigenicity and chemoresistance of HN-CICs. In addition, distinct

Figure 5. Cisplatin resistance and low ROS stress in HN-CICs were mediated by ROS scavenge enzymes. A, HNSCC parental (SAS-P and OECM1-P) cells and HNSCC sphere (SAS-S and OECM1-S) cells were treated with cisplatin for 72 hours. Cell viability of the cisplatin-treated cells was further determined by MTT assay. B, SAS sphere cells were treated with 5, 10, and 20 μmol/L cisplatin, respectively, for 72 hours, then stained with DCFDA. The ROS^{Low} cells in cisplatin-treated HN-CIC cultures were determined by flow cytometry. C, the intracellular level of ROS in SAS-P and cisplatin-resistant (cisPt^R) SAS cells was determined by FACS. D, ALDH activity positive cells (ALDH$^+$) in SAS-P and SAS-cisPt^R cells were measured by FACS analyses (details seen in Materials and Methods). E, differentially expressed genes of ROS scavengers in parental HNSCCs (SAS and OECM1) and sphere cells (SAS-S and OECM1-S) under 2, 3, 5, or 9 weeks of cultivation with defined serum-free selection medium were analyzed and recorded (see Materials and Methods add; ref. 7). F, the expression of ROS scavenger mRNAs in parental HNSCCs (SAS and OECM1) or sphere cells was detected by real-time RT-PCR analysis. To further examine the physiologic effect of cisplatin treatment in combination of scavenger inhibitors on ROS^{Low} or ROS^{High} cells, respectively, SAS sphere cells were either singly treated with cisplatin or cotreated with ROS scavenger inhibitors (2-ME 15 μmol/L or 3-AT 25 mmol/L) for 72 hours; afterward, the percentage of ROS^{Low} cells (G) or ROS^{High} cells (H) was further analyzed. For intracellular ROS content measurement, the drug-treated cells were first stained with DCFDA and then examined by flow cytometry. Data, means ± SD of triplicate samples from three experiments (***, $P < 0.005$). The same concentration (0.03%) of vehicle (DMSO) was added to all control groups.

Published OnlineFirst September 12, 2014; DOI: 10.1158/0008-5472.CAN-14-0626

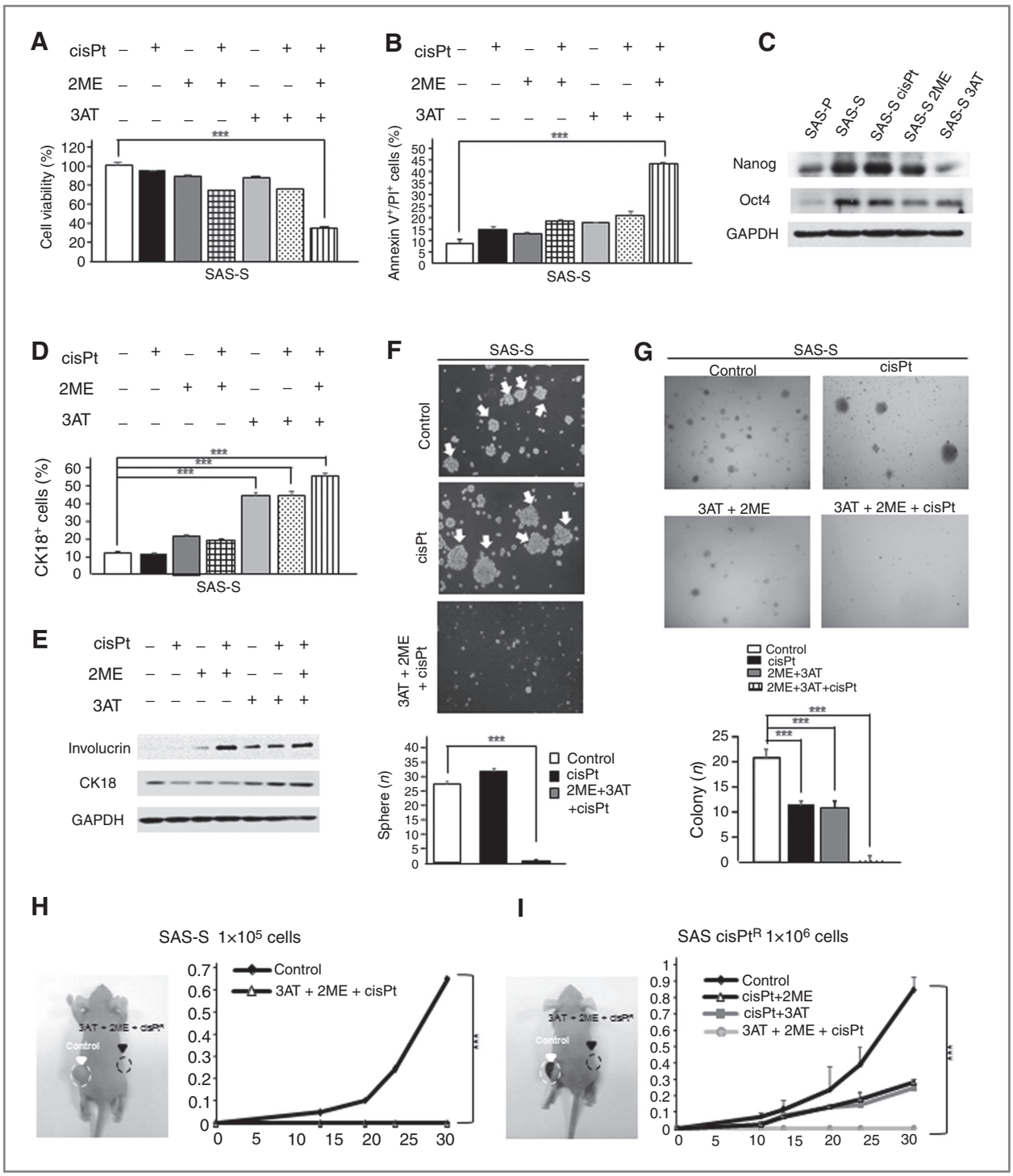

Figure 6. Combined treatment with ROS scavenger inhibitors and cisplatin diminished the cell viability, the sphere formation ability and anchorage-independent growth, and enhanced the cell death and the differentiation ability of HN-CICs. SAS sphere cells were either singly treated with cisplatin or cotreated with ROS scavenger inhibitors (15 μmol/L 2-ME or 25 mmol/L 3-AT) for 72 hours. Afterward, the cell viability (A) and the cells undergoing cell death (B) caused by the drug treatment were further analyzed. For cell viability analysis, the drug-treated SAS sphere cells were further examined by MTT assay (see Materials and Methods). To evaluate the cells undergoing cell death, the drug-treated SAS sphere cells were stained with Annexin V plus PI and then examined by flow cytometry. C, expression of pluripotent stemness proteins (Oct4 and Nanog) in SAS-P–, SAS-S–, cisplatin-treated SAS, 2ME-treated, and 3AT-treated cells was determined by immunoblot analyses. D, the CK18-positive cells with the same treatment was determined by staining drug-treated cells with CK18 antibody and then examined by flow cytometry. (*Continued on the following page.*)

Published OnlineFirst September 12, 2014; DOI: 10.1158/0008-5472.CAN-14-0626

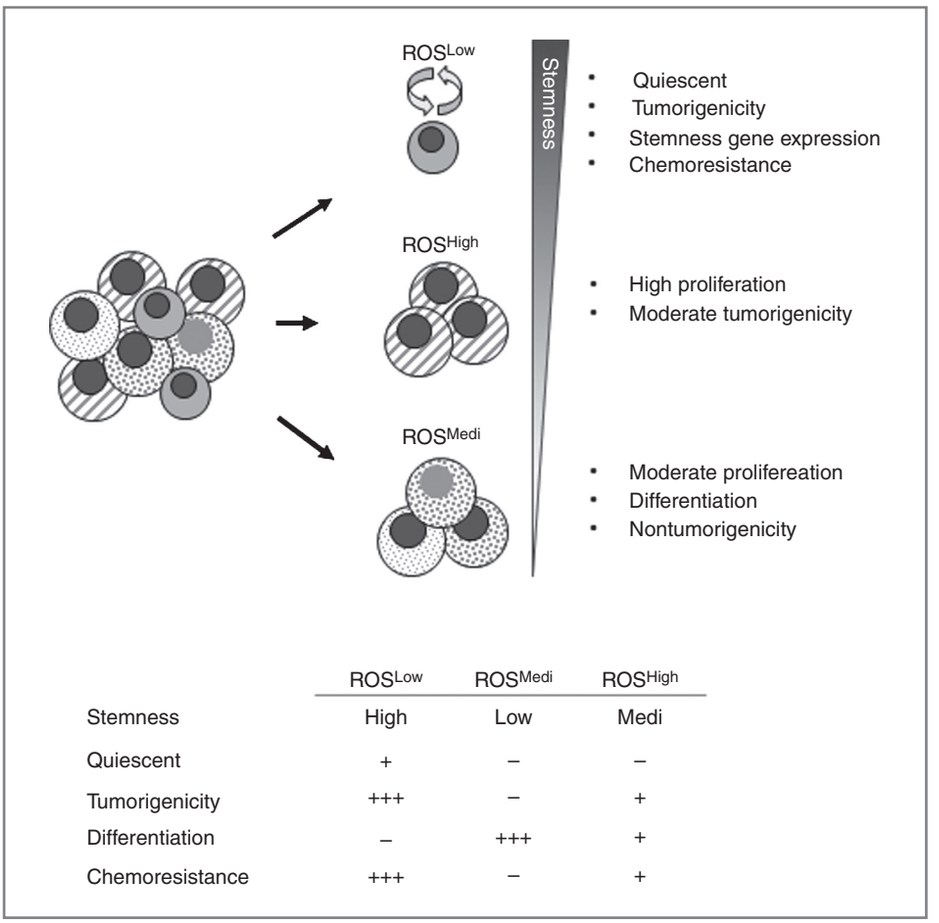

	ROS^{Low}	ROS^{Medi}	ROS^{High}
Stemness	High	Low	Medi
Quiescent	+	–	–
Tumorigenicity	+++	–	+
Differentiation	–	+++	+
Chemoresistance	+++	–	+

Figure 7. Schematic depicts physiologic features of ROS^{Low}, ROS^{High}, and ROS^{Medi} cells related to chemoresistance, stemness properties, tumorigenicity, proliferative activity, etc. Our results (see contexts) indicate that ROS^{Low} cells are in a quiescent state, and possess high tumorigenicity and enhanced stemness properties that may result in the chemoresistance of CICs to chemotherapy. On the other hand, ROS^{High} cells are actively proliferate and more sensitive to therapy and differentiation. Furthermore, the ROS^{Medi} cells exhibit more differentiation and nontumorigenicity.

subpopulation of cells with differential intracellular ROS level in HNSCC exhibit diverse proliferative activity, CIC properties and chemoresistance.

Cells containing ROS-mediated high chemically reactive byproducts are implicated in stress and disease (41). Increasing evidence suggests that low levels of ROS are critical for maintaining the self-renewal and stemness, whereas high levels of ROS effectively shut down self-renewal and confer potent capacity for stem cell differentiation (12, 42). In addition, CICs have similar redox properties as normal stem cell (43). Diehn and colleagues FoxO1 (16) have reported that CD44^{+}CD24^{-} breast CICs have a unique mechanism that protects themselves from ROS through increased antioxidant defenses and unique redox-dependent effects on tumor radioresistance. They also found that the breast CIC-enriched population is associated with genes involved in glutathione synthesis, including Gclm, Gss, and FoxO1. For glioblastoma, it has been reported that glioblastoma stem cells are assumed to constitute a radio-resistant fraction by HIF2α-mediated ROS status (33, 44). However, a relationship between ROS and chemoresistance property in HN-CICs remains elusive. In the present study, we demonstrated that lower ROS levels in HN-CIC–enriched population are associated with increased expression of ROS scavenger such as catalase and SOD2. Pharmacologic depletion of ROS scavengers (SOD2 and/or catalase) in CICs markedly enhanced the cytotoxicity of cisplatin (Fig. 6). Notably, it is evident that catalase and SOD2 has been implicated in chemotherapy resistance of cancer cells (15, 45). On the basis of these findings, we proposed that different CSCs in diverse antioxidant systems have conserved this attribute, which probably helps protect their genomes from ROS-mediated damage. Previous studies also show that signaling molecules

(*Continued.*) E, protein level of epithelial differentiation markers, CK18 and involucrin in drug-treated cells was assessed by Western blot analysis. F, single-cell suspension of SAS sphere cells was treated with cisplatin or cotreated with ROS scavenger inhibitors (2-ME and/or 3-AT) for 72 hours, and the sphere formation ability of drug-treated cells was examined (see Materials and Methods). Arrows, the sphere cells. G, in addition, the abovementioned SAS sphere cells were also plated onto soft agar for 12 day, and the colony formation ability of drug-treated SAS sphere cells was examined (see Materials and Methods). Data, means ± SD of triplicate samples from three experiments (***, $P < 0.005$). Representative images of tumors generated on the recipient nude mice, which were inoculated with drug-treated SAS sphere (H) and SAS cisPt^{R} (I) cells into the subcutaneous space, were photographed (white arrows, control group; black arrows, drug-treated group). Tumor volume was also measured and recorded after inoculation of drug-treated SAS sphere (H) and SAS cisPt^{R} (I) cells in nude mice.

Published OnlineFirst September 12, 2014; DOI: 10.1158/0008-5472.CAN-14-0626

such as FoxOs, APE1/Ref-1, Nrf2, ATM, HIFs, p38, and p53 are involved in the regulation of stem cell self-renewal and differentiation through modulation in antioxidant enzyme systems (11). Therefore, future research delineating the details of what ROS signaling molecules are essential to maintaining stemness properties of CICs in these different cell types are remained to be determined.

CICs in colon, breast, and ovaries have been shown to demonstrate the ability to maintain a quiescent state to evade therapy (46–48). In addition, Dey-Guha and colleagues (49) report that rapidly proliferating cancer cells can produce "G_0-like" progeny through asymmetric division, which are enriched following chemotherapy in breast cancer. These G_0 phase cells show lower intracellular ROS level and exhibit suppressing AKT expression. Herein, we also found that low endogenous ROS status of HNSCCs maintains the quiescent state of CICs. Surprisingly, we observed ROS^{High} cells exhibit the high proliferation index (Fig. 3E and F). Recently, many reports demonstrate that higher ROS state is essential for proliferation of stem/progenitor cells (14, 50). For example, ROS can play roles as second messengers in tightly neural stem cell proliferation and survival by driving PI3K/AKT signaling (24). In addition, it is evident that ROS generation is essential for K-ras–mediated cell proliferation and tumorigenesis in lung cancer (51). On the basis of these findings, we proposed that CIC-enriched populations are partially differentiated due to persistent ROS redox stress on the basis of tumor microenvironment changes, which lead to a heterogeneous mixture of CICs and non-CICs in the tumor. It would be of interest to determine the regulations of these signaling pathways of ROS^{Low} and ROS^{High} HN-CICs, respectively. These studies also suggest that combination of inhibitors for ROS^{Low} and ROS^{High} regulator of the signaling pathway might be more effective compared with blockade of single regulating HN-CICs.

Most conventional anticancer drugs such as cisplatin and 5-fluorouracil are preferentially toxic to proliferating cells, decreases tumor size (52). Herein, we have also confirmed that long-term treatment of cisplatin can enhance the ROS^{Low} cells of CIC properties, and make them prone to survive (Fig. 5D and E). Furthermore, combinatorial treatment of scavenger inhibitors for ROS^{Low} and conventional anticancer drugs reduced the self-renewal ability and survival in HN-CICs (Fig. 5 and 6). In the mean times, it is effective to target the proliferative ROS^{High} cells by long-term treatment of cisplatin (Fig. 5C). Therefore, it will be reasonable that cotreatment with an ROS^{Low} inhibitor along with an ROS^{High} inhibitor as a chemotherapeutic regimen may improve the future treatment of HNSCCs.

Together, this research shows that HN-CICs contain distinct subpopulation cells, and the elevated ROS^{Low} cells in HN-CICs mainly contribute to tumor progression and chemoresistance (Fig. 7). Clinical therapies could perhaps be optimized by overcoming low ROS levels, and identification of regulatory ROS level mechanisms in CICs may be a useful prognostic factor for patients with HNSCC.

Disclosure of Potential Conflicts of Interest

No potential conflicts of interest were disclosed.

Authors' Contributions

Conception and design: Y.-S. Chen, C.-Y. Huang, J.-F. Lo
Development of methodology: C.-W. Chang, Y.-S. Chen, J.-F. Lo
Acquisition of data (provided animals, acquired and managed patients, provided facilities, etc.): Y.-S. Chen, S.-H. Chou, C.-C. Yang, C.-Y. Huang, J.-F. Lo
Analysis and interpretation of data (e.g., statistical analysis, biostatistics, computational analysis): C.-W. Chang, Y.-S. Chen, C.-C. Yang, C.-Y. Huang, J.-F. Lo
Writing, review, and/or revision of the manuscript: C.-W. Chang, Y.-S. Chen, C.-Y. Huang, J.-F. Lo
Administrative, technical, or material support (i.e., reporting or organizing data, constructing databases): Y.-S. Chen, C.-L. Han, Y.-J. Chen, C.-Y. Huang, J.-F. Lo
Study supervision: Y.-S. Chen, Y.-J. Chen, C.-Y. Huang, J.-F. Lo

Acknowledgments

The authors thank Dr. K-W Chang (Department of Dentistry, National Yang-Ming University) for providing critical comments on the article.

Grant Support

This study was supported by grants from the National Science Council (NSC 101N050, 102N031, and 102N446), Taipei Veterans General Hospital (VGHTPE: V102E2-003), and Ministry of Education, Aim for the Top University Plan, National Yang-Ming University (101ACT513 and 102AC-TC14).

The costs of publication of this article were defrayed in part by the payment of page charges. This article must therefore be hereby marked *advertisement* in accordance with 18 U.S.C. Section 1734 solely to indicate this fact.

Received March 4, 2014; revised July 30, 2014; accepted August 19, 2014; published OnlineFirst September 12, 2014.

References

1. Medema JP. Cancer stem cells: the challenges ahead. Nat Cell Biol 2013;15:338–44.
2. Frank NY, Schatton T, Frank MH. The therapeutic promise of the cancer stem cell concept. J Clin Invest 2010;120:41–50.
3. Moore N, Lyle S. Quiescent, slow-cycling stem cell populations in cancer: a review of the evidence and discussion of significance. J Oncol 2011;2011.
4. Koukourakis MI, Giatromanolaki A, Tsakmaki V, Danielidis V, Sivridis E. Cancer stem cell phenotype relates to radio-chemotherapy outcome in locally advanced squamous cell head-neck cancer. Br J Cancer 2012; 106:846–53.
5. Chang CW, Chen CC, Wu MJ, Chen YS, Chen CC, Sheu SJ, et al. Active component of antrodia cinnamomea mycelia targeting head and neck cancer initiating cells through exaggerated autophagic cell death. Evid Based Complement Alternat Med 2013;2013:946451.
6. Haddad RI, Shin DM. Recent advances in head and neck cancer. N Engl J Med 2008;359:1143–54.
7. Chiou SH, Yu CC, Huang CY, Lin SC, Liu CJ, Tsai TH, et al. Positive correlations of Oct-4 and Nanog in oral cancer stem-like cells and high-grade oral squamous cell carcinoma. Clin Cancer Res 2008; 14:4085–95.
8. Chen YS, Wu MJ, Huang CY, Lin SC, Chuang TH, Yu CC, et al. CD133/Src axis mediates tumor initiating property and epithelial-mesenchymal transition of head and neck cancer. PLoS ONE 2011;6:e28053.
9. Wu MJ, Jan CI, Tsay YG, Yu YH, Huang CY, Lin SC, et al. Elimination of head and neck cancer initiating cells through targeting glucose regulated protein78 signaling. Mol Cancer 2010;9:283.
10. Gupta SC, Hevia D, Patchva S, Park B, Koh W, Aggarwal BB. Upsides and downsides of reactive oxygen species for cancer: the roles of

Published OnlineFirst September 12, 2014; DOI: 10.1158/0008-5472.CAN-14-0626

reactive oxygen species in tumorigenesis, prevention, and therapy. Antioxid Redox Signal 2012;16:1295–322.
11. Wang K, Zhang T, Dong Q, Nice EC, Huang C, Wei Y. Redox homeostasis: the linchpin in stem cell self-renewal and differentiation. Cell Death Dis 2013;4:e537.
12. Shi X, Zhang Y, Zheng J, Pan J. Reactive oxygen species in cancer stem cells. Antioxid Redox Signal 2012;16:1215–28.
13. Ogasawara MA, Zhang H. Redox regulation and its emerging roles in stem cells and stem-like cancer cells. Antioxid Redox Signal 2009;11:1107–22.
14. Jang YY, Sharkis SJ. A low level of reactive oxygen species selects for primitive hematopoietic stem cells that may reside in the low-oxygenic niche. Blood 2007;110:3056–63.
15. Achuthan S, Santhoshkumar TR, Prabhakar J, Nair SA, Pillai MR. Drug-induced senescence generates chemoresistant stemlike cells with low reactive oxygen species. J Biol Chem 2011;286:37813–29.
16. Diehn M, Cho RW, Lobo NA, Kalisky T, Dorie MJ, Kulp AN, et al. Association of reactive oxygen species levels and radioresistance in cancer stem cells. Nature 2009;458:780–3.
17. Trachootham D, Alexandre J, Huang P. Targeting cancer cells by ROS-mediated mechanisms: a radical therapeutic approach? Nat Rev Drug Discov 2009;8:579–91.
18. Salnikov AV, Gladkich J, Moldenhauer G, Volm M, Mattern J, Herr I. CD133 is indicative for a resistance phenotype but does not represent a prognostic marker for survival of non-small cell lung cancer patients. Int J Cancer 2010;126:950–8.
19. Volm M, Mattern J. Expression of topoisomerase II, catalase, metallothionein and thymidylate-synthase in human squamous cell lung carcinomas and their correlation with doxorubicin resistance and with patients' smoking habits. Carcinogenesis 1992;13:1947–50.
20. Okumura K, Konishi A, Tanaka M, Kanazawa M, Kogawa K, Niitsu Y. Establishment of high- and low-invasion clones derived for a human tongue squamous cell carcinoma cell line SAS. J Cancer Res Clin Oncol 1996;122:243–8.
21. Barrett CW, Ning W, Chen X, Smith JJ, Washington MK, Hill KE, et al. Tumor suppressor function of the plasma glutathione peroxidase gpx3 in colitis-associated carcinoma. Cancer research 2013;73:1245–55.
22. Flavahan WA, Wu Q, Hitomi M, Rahim N, Kim Y, Sloan AE, et al. Brain tumor initiating cells adapt to restricted nutrition through preferential glucose uptake. Nat Neurosci 2013;16:1373–82.
23. Clay MR, Tabor M, Owen JH, Carey TE, Bradford CR, Wolf GT, et al. Single-marker identification of head and neck squamous cell carcinoma cancer stem cells with aldehyde dehydrogenase. Head Neck 2010;32:1195–201.
24. Le Belle JE, Orozco NM, Paucar AA, Saxe JP, Mottahedeh J, Pyle AD, et al. Proliferative neural stem cells have high endogenous ROS levels that regulate self-renewal and neurogenesis in a PI3K/Akt-dependant manner. Cell Stem Cell 2011;8:59–71.
25. Seale P, Asakura A, Rudnicki MA. The potential of muscle stem cells. Dev Cell 2001;1:333–42.
26. Colter DC, Sekiya I, Prockop DJ. Identification of a subpopulation of rapidly self-renewing and multipotential adult stem cells in colonies of human marrow stromal cells. Proc Natl Acad Sci U S A 2001;98:7841–5.
27. Jones RJ, Collector MI, Barber JP, Vala MS, Fackler MJ, May WS, et al. Characterization of mouse lymphohematopoietic stem cells lacking spleen colony-forming activity. Blood 1996;88:487–91.
28. Gandarillas A, Davies D, Blanchard JM. Normal and c-Myc-promoted human keratinocyte differentiation both occur via a novel cell cycle involving cellular growth and endoreplication. Oncogene 2000;19:3278–89.
29. Li L, Bhatia R. Stem cell quiescence. Clin Cancer Res 2011;17:4936–41.
30. Lin C, Wang H. NADPH oxidase is involved in H2O2-induced differentiation of human promyelocytic leukaemia HL-60 cells. Cell Biol Int 2012;36:391–5.
31. Chou WC, Jie C, Kenedy AA, Jones RJ, Trush MA, Dang CV. Role of NADPH oxidase in arsenic-induced reactive oxygen species formation and cytotoxicity in myeloid leukemia cells. Proc Natl Acad Sci U S A 2004;101:4578–83.
32. Tsai LL, Yu CC, Chang YC, Yu CH, Chou MY. Markedly increased Oct4 and Nanog expression correlates with cisplatin resistance in oral squamous cell carcinoma. J Oral Pathol Med 2011;40:621–8.
33. Kobayashi CI, Suda T. Regulation of reactive oxygen species in stem cells and cancer stem cells. J Cell Physiol 2012;227:421–30.
34. Nagano O, Okazaki S, Saya H. Redox regulation in stem-like cancer cells by CD44 variant isoforms. Oncogene 2013;32:5191–8.
35. Klingelhoeffer C, Kammerer U, Koospal M, Muhling B, Schneider M, Kapp M, et al. Natural resistance to ascorbic acid induced oxidative stress is mainly mediated by catalase activity in human cancer cells and catalase-silencing sensitizes to oxidative stress. BMC Complement Altern Med 2012;12:61.
36. Zhu Z, Mukhina S, Zhu T, Mertani HC, Lee KO, Lobie PE. p44/42 MAP kinase-dependent regulation of catalase by autocrine human growth hormone protects human mammary carcinoma cells from oxidative stress-induced apoptosis. Oncogene 2005;24:3774–85.
37. Siegel R, Naishadham D, Jemal A. Cancer statistics, 2013. CA Cancer J Clin 2013;63:11–30.
38. Maiti AK. Gene network analysis of oxidative stress-mediated drug sensitivity in resistant ovarian carcinoma cells. Pharmacogenomics J 2010;10:94–104.
39. Maiti AK. Genetic determinants of oxidative stress-mediated sensitization of drug-resistant cancer cells. Int J Cancer 2012;130:1–9.
40. Caraglia M, Giuberti G, Marra M, Addeo R, Montella L, Murolo M, et al. Oxidative stress and ERK1/2 phosphorylation as predictors of outcome in hepatocellular carcinoma patients treated with sorafenib plus octreotide LAR. Cell Death Dis 2011;2:e150.
41. Berlett BS, Stadtman ER. Protein oxidation in aging, disease, and oxidative stress. J Biol Chem 1997;272:20313–6.
42. Pervaiz S, Taneja R, Ghaffari S. Oxidative stress regulation of stem and progenitor cells. Antioxid Redox Signal 2009;11:2777–89.
43. Phillips TM, McBride WH, Pajonk F. The response of CD24(-/low)/CD44$^+$ breast cancer-initiating cells to radiation. J Natl Cancer Inst 2006;98:1777–85.
44. Li Z, Bao S, Wu Q, Wang H, Eyler C, Sathornsumetee S, et al. Hypoxia-inducible factors regulate tumorigenic capacity of glioma stem cells. Cancer Cell 2009;15:501–13.
45. Bechtel W, Bauer G. Catalase protects tumor cells from apoptosis induction by intercellular ROS signaling. Anticancer Res 2009;29:4541–57.
46. Gao MQ, Choi YP, Kang S, Youn JH, Cho NH. CD24$^+$ cells from hierarchically organized ovarian cancer are enriched in cancer stem cells. Oncogene 2010;29:2672–80.
47. Dembinski JL, Krauss S. Characterization and functional analysis of a slow cycling stem cell-like subpopulation in pancreas adenocarcinoma. Clin Exp Metastasis 2009;26:611–23.
48. Bao S, Wu Q, McLendon RE, Hao Y, Shi Q, Hjelmeland AB, et al. Glioma stem cells promote radioresistance by preferential activation of the DNA damage response. Nature 2006;444:756–60.
49. Dey-Guha I, Wolfer A, Yeh AC, G Albeck J, Darp R, Leon E, et al. Asymmetric cancer cell division regulated by AKT. Proc Natl Acad Sci U S A 2011;108:12845–50.
50. Yoneyama M, Kawada K, Gotoh Y, Shiba T, Ogita K. Endogenous reactive oxygen species are essential for proliferation of neural stem/progenitor cells. Neurochem Int 2010;56:740–6.
51. Weinberg F, Hamanaka R, Wheaton WW, Weinberg S, Joseph J, Lopez M, et al. Mitochondrial metabolism and ROS generation are essential for Kras-mediated tumorigenicity. Proc Natl Acad Sci U S A 2010;107:8788–93.
52. Kim JJ, Tannock IF. Repopulation of cancer cells during therapy: an important cause of treatment failure. Nat Rev Cancer 2005;5:516–25.

Published OnlineFirst September 12, 2014; DOI: 10.1158/0008-5472.CAN-14-0626

Cancer Research
The Journal of Cancer Research (1916–1930) | The American Journal of Cancer (1931–1940)

AACR American Association for Cancer Research

Distinct Subpopulations of Head and Neck Cancer Cells with Different Levels of Intracellular Reactive Oxygen Species Exhibit Diverse Stemness, Proliferation, and Chemosensitivity

Ching-Wen Chang, Yu-Syuan Chen, Shiu-Huey Chou, et al.

Cancer Res 2014;74:6291-6305. Published OnlineFirst September 12, 2014.